The Impact of Substrate Characteristics on Stretchable Polymer Semiconductor Behavior

*Tianlei Sun, Runqiao Song, Nrup Balar, Pratik Sen, R. Joseph Kline, Brendan T. O'Connor**

Dr. T. Sun, R. Song, N. Balar, P. Sen, Prof. B. O'Connor

Department of Mechanical and Aerospace Engineering, North Carolina State University, Raleigh, NC 27695, USA

Dr. R.J. Kline

Materials Science and Engineering Division, National Institute of Standards and Technology

Gaithersburg, MD 20899, USA

KEYWORDS Stretchable electronics, Polymer semiconductors, Yield strain, Deformability, Adhesion energy

Abstract: Stretchable conductive polymer films are required to survive not only large tensile strain but also stay functional after the reduction in applied strain. In the deformation process, the elastomer substrate that is typically employed plays a critical role in the response of the polymer film. In this study, we examine the role of a PDMS elastomer substrate on the ability to achieve stretchable PDPP-4T films. Specifically, we consider the adhesion and near surface modulus of the PDMS tuned through UV/ozone treatment on the competition between film wrinkling and

plastic deformation. We also consider the role of PDMS tension on the stability of films under cyclic strain. We find that increasing the near-surface modulus of the PDMS and maintaining the PDMS in tension throughout the cyclic strain process promotes plastic deformation over film wrinkling. In addition, the UV/ozone treatment increases film adhesion to the PDMS resulting in significantly reduced film folding and delamination. For 20 min UV/ozone treated PDMS, we show that a PDPP-4T film RMS roughness is consistently below 3 nm for up to 100 strain cycles with a strain range of 40 %. In addition, while the film is plastically deforming, the microstructural order is largely stable as probed with grazing incidence X-ray scattering and UV-visible spectroscopy. These results highlight the importance of the neighboring elastomer characteristics on the ability to achieve stretchable polymer semiconductors.

1. Introduction

Combining stretchability with electronic functionality is poised to advance technologies such as health monitoring and soft robotics as well as open up new technologies previously unachievable due to mechanical limitations of conventional inorganic semiconductors.[1,2] There are a number of approaches used to achieve stretchable devices that include the use of geometric structures that limit the strain on the active layers under large global deformation,[3,4] and intrinsic methods where the electronic materials are able to withstand large deformation and remain functional.[5-11] One promising strategy is to use highly deformable polymer conductors that can be seamlessly integrated into stretchable objects. To achieve stretchable polymer semiconductor films, methods have included using cracked film networks,[12] polymer-elastomer blends,[2,5-7] cross-linked polymers,[8,9] and viscoelastic polymers.[10,11,13] The use of viscoelastic polymer semiconductors that can be cyclically strained while maintaining microstructural order provides

one promising strategy to achieve intrinsically stretchable devices. Here, the neighboring elastomer provides the driving force for the deformation of the semiconductor, which deforms in both tension and compression while maintaining stable electrical characteristics.[8,14-16] In this approach, the mechanical behavior of the polymer can be optimized through polymer design,[13, 17-20] as well as through the use of additives or polymer blending.[2,11,21] In many of the demonstrations of stretchable polymer semiconductors, results are provided for films only under tensile strain.[10] If the films are strained multiple times, the films characteristics at the low strain limit are often not considered in detail.[18,19] In the cases where they are characterized and reported, film wrinkling, folding, and delamination can often be observed.[9,13] If neat polymer semiconductor films are to be successful in stretchable applications, it is important to understand the mechanical failure mechanisms that include the formation of film discontinuities, film wrinkling and delamination, or extensive morphological changes that can occur during stretching events.

In this paper, we consider the characteristics of the neighboring elastomer on the ability to cyclically stretch a polymer semiconductor film in a repeated manner without mechanical failure (no cracking, wrinkling, folding or delamination) and minimal morphological degradation. The focus of this investigation is on the role of adhesion between the elastomer and the polymer film, and the stiffness of the underlying elastomer. We consider the polymer semiconductor poly[2,5-bis(2-octyldodecyl) pyrrolo[3,4-c] pyrrole-1,4 (2H,5H)-dione-3, 6-diyl) –alt-(2,2';5',2''; 5'',2'''-quaterthiophen -5,5'''-diyl)] (PDPP-4T) (**Figure 1(b)**) on a polydimethylsiloxane (PDMS) elastomer substrate. PDPP-4T is chosen as it has been reported to possess a high field effect charge mobility,[22-24] and has a glass transition temperature below room temperature (shown in **Figure S1**). While DPP-4T is semicrysalline as discussed below, the rubbery state of the

polymer at room temperature results in a ductile film, and we have measured a crack onset strain of over 80 % when strained on PDMS. The PDMS elastomer was selected as the substrate due to its large extensibility, good chemical resistance, thermal stability, and wide use in stretchable organic electronics. PDMS is also widely applied in thin film mechanical characterization.[25,26] The PDMS surface energy, and near surface stiffness can also be effectively modulated through UV/ozone (UVO) treatment.[27-31] The changes in the stretched films were then probed by UV-visible spectroscopy and atomic force microscopy (AFM) using a strain stage that can be integrated with both instruments for quasi in-situ characterization. The film morphology was also probed with grazing incidence wide-angle X-ray scattering (GIWAXS).

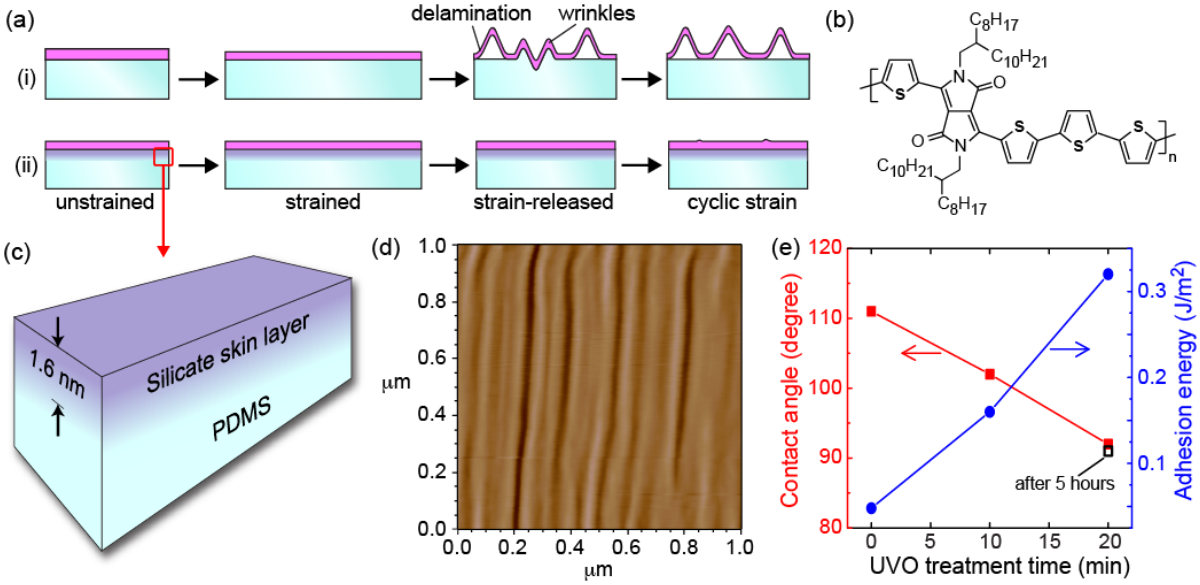

Figure 1. (a) Illustration of cyclically strained polymer film when on an (i) untreated PDMS substrate and (ii) UVO treated PDMS substrate. (b) The molecule structure of PDPP-4T. (c) An illustration of the UVO treated PDMS substrate with a silicate skin layer, showing approximate thickness of the silicate layer for 20 min UVO treatment. (d) AFM image of surface wrinkling for a 20 min UVO treated PDMS under compression. (e) Water contact angle on PDMS and

adhesion energy between 30 nm-thick PDPP-4T films and PDMS with different UVO treatment time.

We find that increasing the elastic modulus of the near surface PDMS and the increase in adhesion energy between the PDMS and PDPP-4T results in improved deformation stability of the PDPP-4T films under cyclic strain, as illustrated in **Figure 1(a)**. Holding the PDMS substrate in tension throughout the applied strain cycle can also be used to achieve stable deformation by promoting plastic deformation over wrinkling. We show that the PDPP-4T film can be cyclically strained by approximately 40 % up to 100 times while showing stable surface roughness and stable morphological order. As part of this work, it is shown that while there is no film wrinkling over the strain range considered, this does not equate to being within the film's elastic strain limit, but rather that the polymer film yields prior to reaching the critical stress required for wrinkling. While plastic deformation occurs, the charge mobility was found to change in a predictable fashion based on the average in-plane orientation of the polymer.

2. Results and Discussion

2.1 PDMS Properties

The PDMS substrate surface energy, and near surface stiffness was modulated through UVO treatment. When exposed to UVO, the methyl groups of PDMS are converted into hydroxyl groups and eventually converts the CH_3-Si-O- structure into a hydrophilic silicate network at the PDMS surface [as shown **Figure 1(c)**].[29] This transformation increases the PDMS surface energy,[27-29] and the near surface stiffness.[28,30,31] The UVO treatment of PDMS also results in embrittlement of the surface due to the silicate formation. An untreated PDMS substrate can be strained by over 100 % prior to rupture. With UVO treatment, applied strain can result in surface

cracks forming in the silicate layer resulting in a lower PDMS rupture strain. However, under limited UVO treatment, the surface retains elastomeric properties and the PDMS can be strained significantly without crack formation. In our case, when the PDMS is treated in a ventilated UVO chamber for 20 min, surface cracks will appear at strains of approximately 70 %. At strains less than 70 % the PDMS can be cyclically strained without crack formation. Thus, the UV/ozone treatment times were limited to 20 minutes in this study. This approach to manage the substrate stiffness was chosen over varying cross-linker ratio as the variation in elastomer stiffness is expected to be significantly greater with UVO treatment than a reasonable increase in cross-linker density.[32]

To determine the increase in surface stiffness of the PDMS with UVO treatment we applied a wrinkling based metrology method.[27,30] This approach is based on the interfacial instability generated from the modulus mismatch between a film on a more compliant substrate when under compression. This instability results in wrinkling with a characteristic wavelength (λ), where the elastic modulus of the thin film can be determined by

$$E_f = 3E_s\left(\frac{1-\nu_f^2}{1-\nu_s^2}\right)\left(\frac{\lambda}{2\pi h}\right)^3, \quad (1)$$

where E is the elastic modulus, ν is the Poisson ratio, and h is the thin film thickness. The subscripts f and s are for the film and substrate, respectively.[25] The elastic modulus of the PDMS substrate (E_s) was determined to be 0.81 MPa by performing a tensile test on an untreated PDMS substrate, ν_f and ν_s are taken as 0.33 and 0.5, respectively.[25] To generate the wrinkles the PDMS was strained by 15 % and then treated with UVO for 20 min. The PDMS was then compressed until surface wrinkles were formed. The average wavelength of the wrinkles was measured using atomic force microscopy (AFM), shown in **Figure 1(d)**, and was determined to be approximately 63 nm. The thickness of the surface layer is measured using variable angle spectroscopic

ellipsometry (VASE). While, it is expected that there is a gradient in the silicate concentration with depth, we apply a simple 2 layer model.[31] Using this approach, *h* was determined to be 1.6 nm, with the model fit given in **Figure S2**. This results in an estimated surface modulus of the UVO treated PDMS of 570 MPa. Previous reports of the modulus of the silicate layer on PDMS formed with UV/ozone or O_2 plasma have ranged from 120 MPa to 1.5 GPa.[30,33,34] Here, we find the modulus to be consistent with these previous estimates. Nevertheless, our reported modulus should be taken as an approximate value given that a gradient in modulus with depth into the PDMS should exist, and due to a large compressive strain of approximately 10 % used to observe the surface wrinkles. The elastic modulus of the PDPP-4T films was determined using the same wrinkling approach and was found to be 330 MPa for a 150 nm thick film and 140 MPa for a 30 nm thick film. Thus, the increase in the near surface PDMS modulus increases the effective modulus of the substrate and acts to decrease the modulus mismatch between the PDPP-4T film and PDMS, which will impact the PDPP-4T fracture strain,[35] and wrinkling behavior as discussed further below.

The silicate formation will also impact the surface energy of the PDMS and adhesion to the polymer semiconductor. The change in surface energy of PDMS under different UVO treatment conditions was characterized with static water contact angle measurements. The contact angle results are shown in **Figure 1(e)** for untreated PDMS and under UVO treatment for 10 min and 20 min. As expected, the contact angle drops with increasing treatment time, indicating an increase in surface energy. In UVO treated PDMS, hydrophobic recovery of the surface is known to occur.[29] In our case, the water contact angle of the 20 min UVO treated PDMS was measured 5 h after treatment and the contact angle showed negligible change (**Figure 1(e)**). The stable contact angle suggests the hydrophobic recovery of the treated PDMS does not happen with any

significance over this time period. Thus all experiments with PDMS occurred within 5 h of UVO treatment allowing the film behavior to be studied without considering hydrophobic recovery of the PDMS surface. The adhesion energy between PDPP-4T film and PDMS substrate was determined by 90º peel tests with results shown in **Figure 1(e)**. The adhesion energy for PDPP-4T thin film onto neat PDMS is found to be 0.048 Jm^{-2}, which is consistent with previous results of polymer thin films on PDMS.[36] The adhesion energy increases to 0.16 J m^{-2} and 0.32 J m^{-2} with 10 min and 20 min UVO treatment, respectively. While UVO treatment is used here to modulate substrate stiffness and adhesion, for long term stable operation alternative strategies to manage these properties would be required. Modulating adhesion may be possible through grafting monolayers onto the elastomer,[37] while modulating stiffness may be possible through elastomer selection or through elastomer nano-composite design.[38]

2.2 Competition Between Wrinkling and Plastic Deformation

As shown above, when a thin film is compressed while on an elastomer substrate, surface wrinkles typically appear. In fact, this wrinkling behavior has been exploited as a means to achieve stretchable devices.[3,39] In these demonstrations, the film is kept within its elastic limit and the applied strain is restricted to a range of stable wrinkle formation. Here, we regard wrinkle formation as undesirable behavior. This approach limits the acceptable strain-range and significant out of plane wrinkling may limit device designs and applications where contact to nominally smooth surfaces is necessary. In addition, after the wrinkles have formed, continued compression results in stresses that promote film delamination.[40] Alternatively, plastic deformation of the thin film may occur rather than film wrinkling under certain conditions. Here, we are interested in understanding the competition between film wrinkling and yielding.

It has been previously proposed that the yield strain of a polymer thin film can be found by placing the film on an elastomer and cyclically straining the film/elastomer composite over increasing strain ranges until wrinkles are observed when the strain is removed.[41] It was argued that over the elastic regime, the strained film and substrate both return to their original shape without wrinkling. Past the yield point, the film is plastically deformed and when the applied strain is removed, a compressive force will act upon the plastically deformed film resulting in film wrinkling.[5,13,41] While this is true, there is also a competing mechanism of plastic deformation of the film. If the yield strength is met prior to the critical stress required for film wrinkling then plastic deformation would be favored. To consider this competition between yielding and wrinkling, the PDPP-4T film is laminated onto a PDMS substrate while both being in an unstrained state. The film/PDMS composite is then strained to a specified strain and returned to the unstrained state. The surface is then measured by AFM to determine if wrinkles have formed. If no wrinkles or folds are found, the measurement is repeated with a larger applied tensile strain. Note that film folding is a competing process where the out of plane buckling of the film is more localized.[42] For thin films under compression film folding may be found rather than wrinkles. We do not distinguish between the two here given that both represent film moving out of the surface plane. We refer to the strain that is applied that results in wrinkle (or fold) formation upon strain removal as the wrinkle onset strain. This approach is similar to that previously described by Printz et al. who used light diffraction as the wrinkle onset probe.[41] The wrinkle onset strain for 30 nm and 150 nm thick PDPP-4T films, on various UVO treated PDMS is given in **Figure 2**. AFM images of the films just prior to reaching, and just after reaching the wrinkle onset strain are given in **Figure S3**. For the 150 nm and 30 nm thick film, the wrinkle onset strain was approximately 15 % and 17 % respectively, when on the untreated PDMS. The

wrinkle onset strain then increased with UVO treatment of the PDMS substrate. For the 30 nm thick film the wrinkle onset strain was 40 % for 10 min UVO-treated PDMS and increased to 48 % for 20 min UVO-treated PDMS. The wrinkle onset strain for 150 nm film followed the same trend but with overall lower values. It is important to note that since the wrinkles will relax over time given the viscoelastic nature of the DPP-4T, consistent with a recent report on wrinkle relaxation.[43] It was found that DPP-4T wrinkles that would form by placing the film/elastomer composite in compression would relax after several hours. Thus, these AFM images were measured immediately after the strain even, typically within approximately 20 minutes.

These results demonstrate that the substrate plays a large role in the wrinkle onset behavior. To highlight the substrate's effect, we also determined the contraction of a strained PDPP-4T film after removing the film from the PDMS substrate. This was done by straining the film while on PDMS, transferring the film to a second substrate and then floating the film onto water. Once removed from the substrate, the contraction of the film [(strained film length – final length)/unstrained film length] was measured. The contraction of the film captures the residual elastic strain in the film, and can be considered an approximation of the yield strain.[44,45] We find that for films strained by 50 % then floated off in water, the contraction of the film was approximately 4 %, independent of the film thickness and PDMS substrate, as shown in **Figure 2**. This suggests that the yield strain of PDPP-4T films is approximately 4 %, and highlights the intrinsic behavior of the film rather than the influence of the substrate. Note that during this experiment, the strained PDPP-4T film will undergo stress relaxation indicated by wrinkle relaxation over time mentioned above, and stress relaxation will reduce the elastic contraction observed. However, the film was transferred off PDMS and floated on water immediately after

deformation and stress relaxation is expected to be small. From these tests, we can conclude that wrinkling onset strain does not necessarily capture the yield strain of the film.

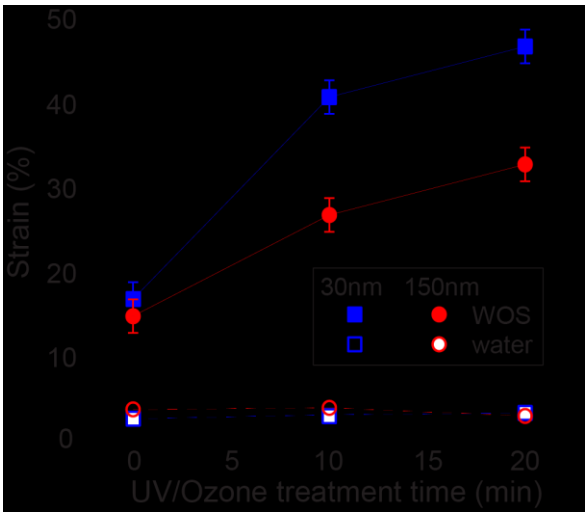

Figure 2. Tensile strain applied to the PDPP-4T/PDMS composite that results in surface wrinkling when the applied strain is removed, which we refer to as the wrinkle onset strain (WOS). The graph also includes the contraction of films strained by 50 % and then floated off in water (water).

To understand the competition between wrinkling and plastic deformation, it is instructive to return to the equation governing bending a film on a more compliant substrate. By conducting a force balance, the critical stress (σ_w) to induce wrinkling is given by,[25]

$$\sigma_w = (\frac{9}{64}\bar{E}_f\bar{E}_s^2)^{\frac{1}{3}}. \quad (2)$$

Equation 2 is based on linear elastic mechanics for both the film and substrate. We can compare this critical stress to the yield strength to determine which would occur first. As a simple approximation, the yield strength (σ_y) can be estimated by assuming the film behaves linear-elastically up until its yield point ($\sigma_y = \bar{E}_f\varepsilon_y$). Under a compressive strain, the competition

between σ_y and σ_w is plotted in **Figure 3(a)**, based on the elastic modulus mismatch between the film and substrate and the film yield strain. For most polymer films, such as PDPP-4T on PDMS, the elastic modulus mismatch results in wrinkling occurring prior to yielding in typical wrinkling metrology tests.[25] The elastic modulus of most polymer semiconductor films are between 100 MPa to 3 GPa whereas the underlying PDMS elastomer is ≈ 1 MPa.[35,46] This would result in a film to substrate modulus ratio of 100 to 3,000 resulting in wrinkling occurring prior to plastic deformation for films with yield strains greater than a couple percent. However, we propose that the yield strength can be reached prior to the critical stress for wrinkling if the film/substrate composite is first strained significantly in tension, as illustrated in **Figure 3(b)**. This is due to several contributing factors that include a reduction in film stiffness and compressive yield strength, along with an increase in substrate stiffness.

First, consider the behavior of the polymer thin film under large tensile strain. It has been shown that the elastic modulus of polymer films can change significantly when strained in tension.[36,39] For the 150 nm thick PDPP-4T film strained by 45 %, we found that the elastic modulus dropped by approximately 30 %, and remained at this lower elastic modulus when the film was strained to 60 %. This was determined using a previously described wrinkling metrology approach where the strained film is transferred to a lightly strained PDMS substrate and then placed in compression.[47] These results are consistent with previously measured strain-oriented poly(3-hexylthiophene) (P3HT), which showed a roughly 50 % drop in elastic modulus for films strained by 50 %.[47] A complimentary effect is that in a polymer strained past its yield point, its yield strength in compression can be lower than the yield strength of an unstrained film, associated with the Bauschinger effect.[45] The relative drop in compressive yield strength for

strain oriented PDPP-4T films requires further analysis. However, a 50 % drop in compressive yield strength has been observed in oriented polycarbonate and polypropylene.[45,48]

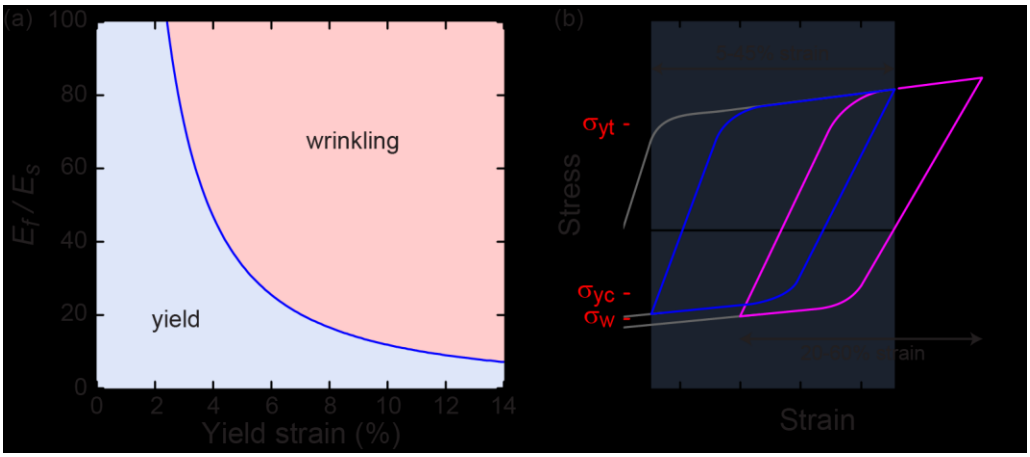

Figure 3. (a) The dependence on the elastic modulus ratio between the film (E_f) and substrate (E_s) on the competition between film yielding or wrinkling when placed under compression, given as a function of yield strain. (b) An illustration of the possible stress-strain behavior of the thin films under a strain range of 5 % - 45 % strain and 20 % - 60 % strain range. Also included is the yield of the unstrained film (σ_{yt}), the yield strain of the 45 % strained film upon strain removal (σ_{yc}), and the critical strain for wrinkling (σ_w).

In addition to the thin film, the behavior of the elastomer substrate under large tensile strain will also impact the competition between yielding and wrinkling. The critical stress for wrinkling given by equation (2) is derived by invoking Winkler's foundation for the force imparted by the substrate on the thin film.[25] Winkler's foundation assumes linear force-deflection relationship, and introduces the elastic modulus of the substrate to capture the out-of-plane stiffness of the elastomer. When the elastomer is strained in tension, the out of plane stiffness can increase significantly.[49,50] Even relatively low uniaxial strains of 10 % can result in almost a doubling of

the stiffness of PDMS in the transverse direction.[49] While this behavior will depend on details of the PDMS such as the degree of crosslinking, it highlights that the film to substrate stiffness ratio decreases significantly when the composite is under tensile strain. The increase in out-of-plane stiffness of the substrate results in a larger critical stress for wrinkle formation, per equation (2). Furthermore, it is expected that this change in out of plane stiffness will be enhanced with UVO treatment. Thus, in highly strained films, there is a reduction in the film/substrate modulus ratio that occurs simultaneously with a possible decrease in yield strength of the film, resulting in film yielding being increasingly favored over wrinkle formation. Assuming a nominal compressive yield strain of 4 % for the 30 nm thick PDPP-4T film, a modulus ratio of the film to substrate less than 47 will results in plastic deformation prior to wrinkling under the simple linear elastic approximation. Ignoring the drop in elastic modulus and likely drop in yield strength of the strained PDPP-4T film, this could be achieved if the out of plane stiffness of the PDMS increased to 2.6 MPa. Given that the modulus of the PDMS was 0.8 MPa in the unstrained state, and for the 20 min UVO treated PDMS there is a thin silicate layer with a modulus of 570 MPa, this out of plane stiffness is likely to be achieved in moderately strained PDMS.

In a highly strained film/elastomer composite where the strain is being reduced, if the film's yield strength is met prior to the critical stress for wrinkling, then the film will plastically deform and strain hardening is expected. Strain hardening will increase the stress in the film and promote film wrinkling (see **Figure 3(b)**). At the same time, as the strain is removed, the PDMS out of plane stiffness decreases. These combined effects will result in film wrinkling at some point in the strain release process. The lower strain limit of this behavior is then the wrinkle onset strain observed in **Figure 2**. The observed difference in wrinkle onset strain for the thin and thick PDPP-4T films may be attributed to the difference in elastic modulus of the films, which is

consistent with these arguments. In addition, the films may have different strain hardening behavior under compression due to greater surface confinement effects in the thin film.[5]

In addition to film wrinkling, film folding and delamination are competing mechanism under cyclic strain. The UVO treatment not only increases the stiffness of the PDMS surface, it also increases the adhesion between the film and PDMS (**Figure 1(e)**), which increases the crack onset strain and reduces delamination. Under tensile strain, a large adhesion energy is believed to increase the crack onset strain by ensuring a uniform strain is applied across the film reducing stress concentration points and localized necking.[51,52] During the strain release process, the substrate forces the thin film to compress until the strain energy release rate exceeds the interfacial toughness resulting in localized delamination.[53] Increasing the adhesion energy improves the interfacial toughness delaying the onset of delamination. The competition between wrinkling and delamination has been considered in detail by Nolte et al.[40] For the sample conditions given here, the measured adhesion is strong enough that wrinkle will be favored over immediate delamination.[40] However, once wrinkles form, the stored energy upon further compression may be released through film folding or delamination.[40,42] Under cyclic loading, the irreversible plastic deformation process is expected to results in stresses that promote delamination and folding and these competing failure mechanism must also be considered.

2.3 Film Morphology Under Cyclic Strain

The wrinkle onset strain provides guidance on the strain range over which the film is expected to plastic deform in a stable manner. However, it does not capture the cyclic stability of the film in terms of wrinkling, folding, delamination, or film morphology. In this section, the stability of the film under cyclic strain is considered. Two strain ranges were considered in detail, an engineering strain range from 5 % to 45 % and from 20 % to 60 %, with the strain

values given with respect to the unstrained state. The strain limit of 45 % was chosen as it is within the wrinkle onset limit only for the film on the 20 min UVO treated PDMS. The lower strain limit of 5% is chosen for two primary reasons. First, the tension of the PDMS at this strain limit allows the films to be probed by AFM while being on the strain stage. In addition, it holds the PDMS in slight tension ensuring the wrinkle onset strain is not met for the film on 20 minute UVO treated PDMS. An illustration of this strain range and the competing yield stress and critical stress for film wrinkling is provided in **Figure 3(b)**. A cyclic strain range from 20 % to 60 % is also considered. In this case, a 60 % tensile strain is beyond the wrinkle onset strain for all substrate conditions. It is chosen as it approaches the upper limit of strain allowed by the UVO treated PDMS. Given that 60 % strain is above the nominal wrinkle onset strain, the appearance of wrinkling occurs when the strain is dropped below 20 %. By setting the lower strain limit as 20%, the film is maintained in a region that favors plastic deformation over film wrinkling for the 20 UVO treated PDMS case. This strain range is also illustrated in **Figure (3b)** and provides support that maintaining the film with a stable plastic deformation zone enables stable stretchable film behavior.

The changes in surface topography of the 30 nm-thick PDPP-4T films under cyclic strain are summarized in **Figure 4** and **Figure S4**. Before the film/PDMS composite was strained, the film surfaces were smooth with an RMS roughness of ≈ 1 nm, based on 5 μm x 5 μm AFM scans. Under cyclic strain, the films remained relatively smooth at the high strain limit with RMS roughness below 3 nm for all PDMS substrates considered (**Figure S4**). However, at the lower strain limit, the surface roughness had a strong dependence on the PDMS UVO treatment conditions. For a film on untreated PDMS, wrinkling followed by delamination occurs

immediately upon the first decrease in applied strain. As the strain cycles continue, delamination became more severe and film roughness increased significantly.

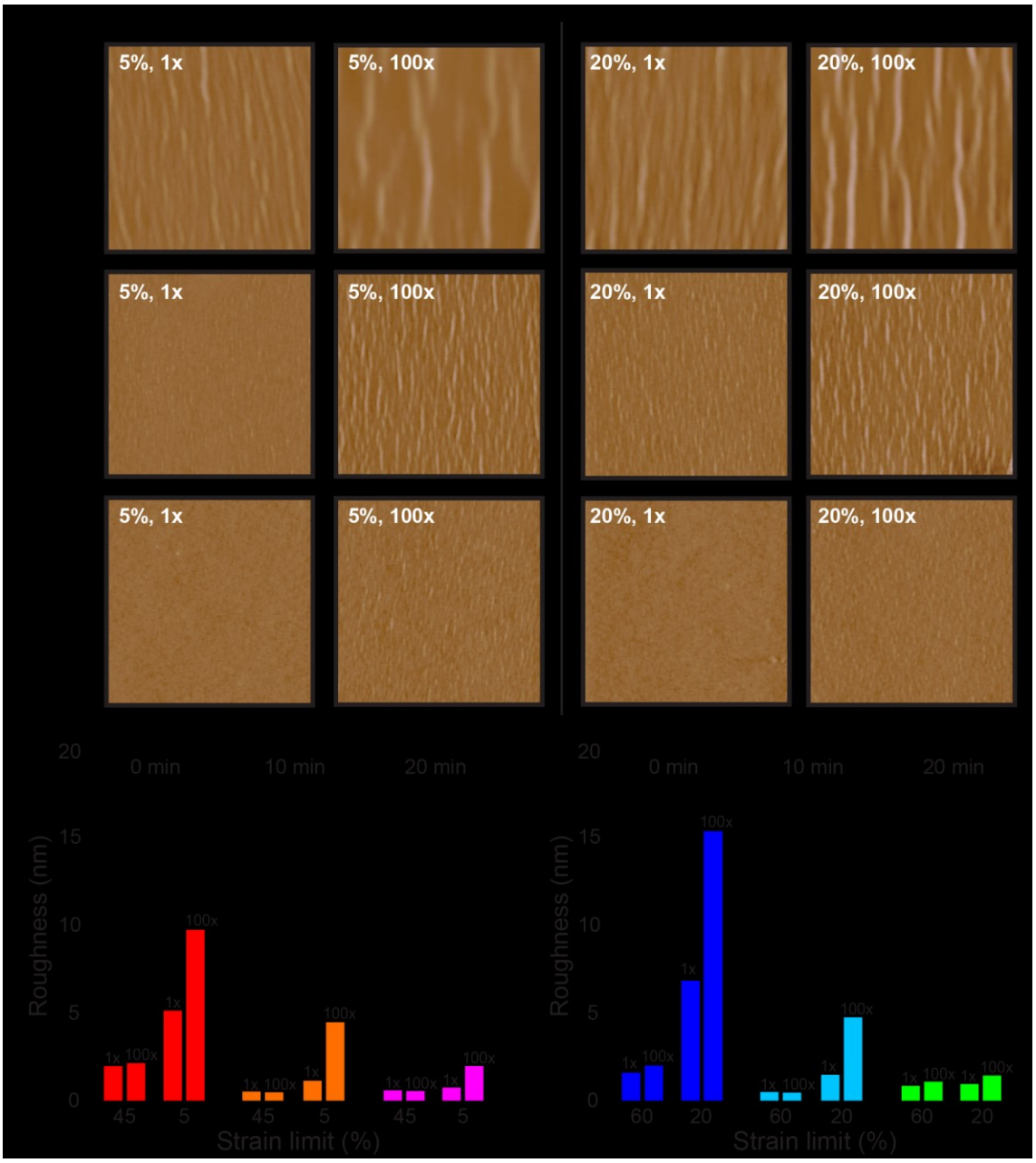

Figure 4. (a) AFM images of 30 nm-thick films being strained over two different strain ranges and held at the lower strain limit. The lower limit of 5 % is for films strained between 5 % and 45 %, and the lower limit of 20 % is for films strained between 20 % and 60 %. Images are

provided for 1 and 100 strain cycles and on PDMS with different UVO treatment conditions. All images are 5 μm x 5 μm. The RMS roughness determined from the AFM images for films (b) strained between 5 % and 45 %, and (c) films being strained between 20 % and 60 %.

The RMS roughness of the films under cyclic strain reduced significantly when on UVO treated PDMS. For 10 min UVO treated PDMS, wrinkling features were barely visible after the first strain cycle, but wrinkling/folding and delamination increased with cyclic strain. This is characteristic of fatigue failure, where repeating strain continuously weakens the interfacial bonds until delamination occurs. When the UVO treatment increases to 20 min, the film RMS roughness remains approximately 2 nm even after 100 strain cycles. The topography of the film at 10, 30, and 50 strain cycles for the 20 min UVO treated PDMS condition are given in **Figure S4**, showing stable surface roughness with strain cycle. This behavior correlates well with the increase in the wrinkle onset strain and increased adhesion energy with UVO treatment of PDMS.

Under cyclic strain the films were found to plastically deform in both tension and compression. But, in addition to avoiding wrinkling and delamination, it is important that the microstructural order of the films is maintained during this process. To capture changes in microstructural order of the polymer under cyclic strain, the films were probed by UV-vis spectroscopy and GIWAXS. The UV-visible spectroscopy was conducted with linear polarized light to measure the dichroic ratio of the films with strain. When the films are strained, increasing dichroism is associated with the alignment of the polymer backbones along the direction of strain.[14] For the strained PDPP-4T films, we found that the increase in dichroic ratio was largely linear with applied strain, and independent of the UVO treatment of the PDMS, as shown in **Figure S5**. Upon strain release, the

dichroic ratio was found to reduce, dropping slightly more quickly than the increase under tension. The dichroic ratio under cyclic strain was also monitored and was found to consistently repeat with strain cycle independent of the PDMS substrate, as shown in **Figure 5(a)** and **Figure S5**. Finally, the absorbance features for films under the first strain cycle and after 100 strain cycles are compared in **Figure 5(b)** and **Figure S6**. The PDPP-4T films absorb light over a range wavelength from 400 nm to 1,000 nm, with an absorption peak at 784 nm and a shoulder at 700 nm indicative of H-aggregation (**Figure 5(b)**).[54] The strength of the vibronic feature at 700 nm are relatively weak suggesting that the films were not highly ordered after spin coating. This is attributed to the films being spun cast from low boiling point solvent and without subsequent thermal annealing. However, it is observed that the absorbance features remains similar throughout the strain cycles suggesting that while the polymer chains are orienting in the direction of strain, the local polymer order in the film is retained. This is consistent with previous measurements of plastically deformed polymer semiconductor thin films.[14,16]

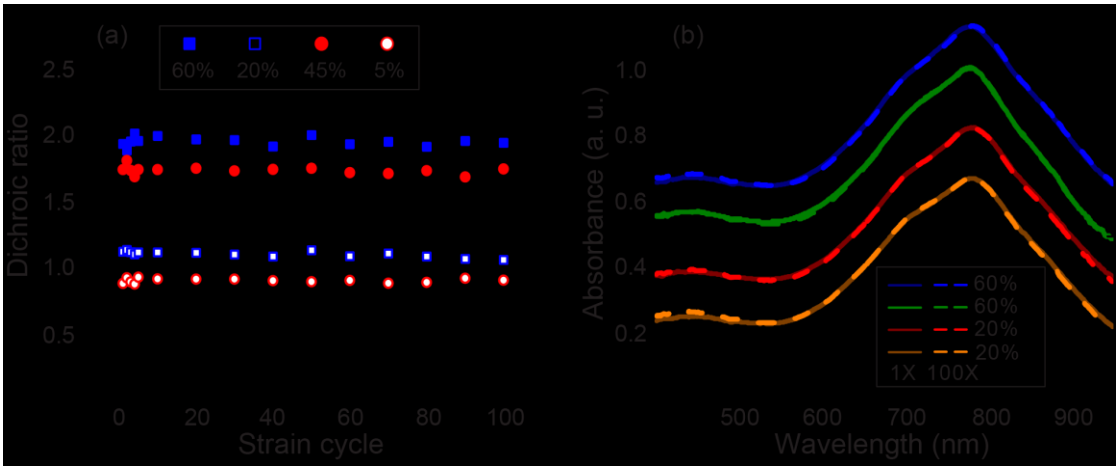

Figure 5. (a) The dichroic ratio of 30 nm thick DPP-4T films on 20 min UVO treated PDMS at the strain limits of 5 % - 45 % and 20 % - 60 % with increasing strain cycles. The dichroic ratio was taken at 783 nm. (b) The normalized absorbance of films on 20 min UVO treated PDMS

substrates that have been cyclically strained between 20 % and 60 % and held at their respective strain limits. The absorbance after the first strain cycle (1x) is compared to 100 cycles (100x). The measured absorbance are normalized and offset for clarity.

To probe the crystalline packing behavior of the film under cyclic strain, 2D GIWAXS images of the 30 nm thick films were taken with the X-ray beam nominally parallel and perpendicular to the strain direction, provided in **Figure 6**. Here, we consider the 20 % to 60 % strain range. 2D GIWAXS image of an unstrained film is also provided in **Figure S7**. It is found that as the film was strained the polymer backbone aligns in the direction of strain. When the strain is reduced to the 20 % strain limit, the in-plane anisotropy decreases. These measurements are consistent with UV-vis spectroscopy measurements. Interestingly, (h00) diffraction peaks becoming more intense out of plane than in-plane with increasing strain cycle. In-plane and out-of-plane section cuts from the 2D images are provided in **Figure S8** clearly showing this change in out-of-plane packing. The origin of this behavior is not understood at this time but may be due to stress relaxation associated with minimizing the in-plane spacing of polymer chains upon compression, or due to more active slip systems in face-on crystals.[55,56] Given that the films are biaxially anisotropic, it is difficult to determine changes in film crystallinity without full reciprocal space maps. However, the 2D images suggest there was not a large change in crystallinity, consistent with the absorbance behavior.

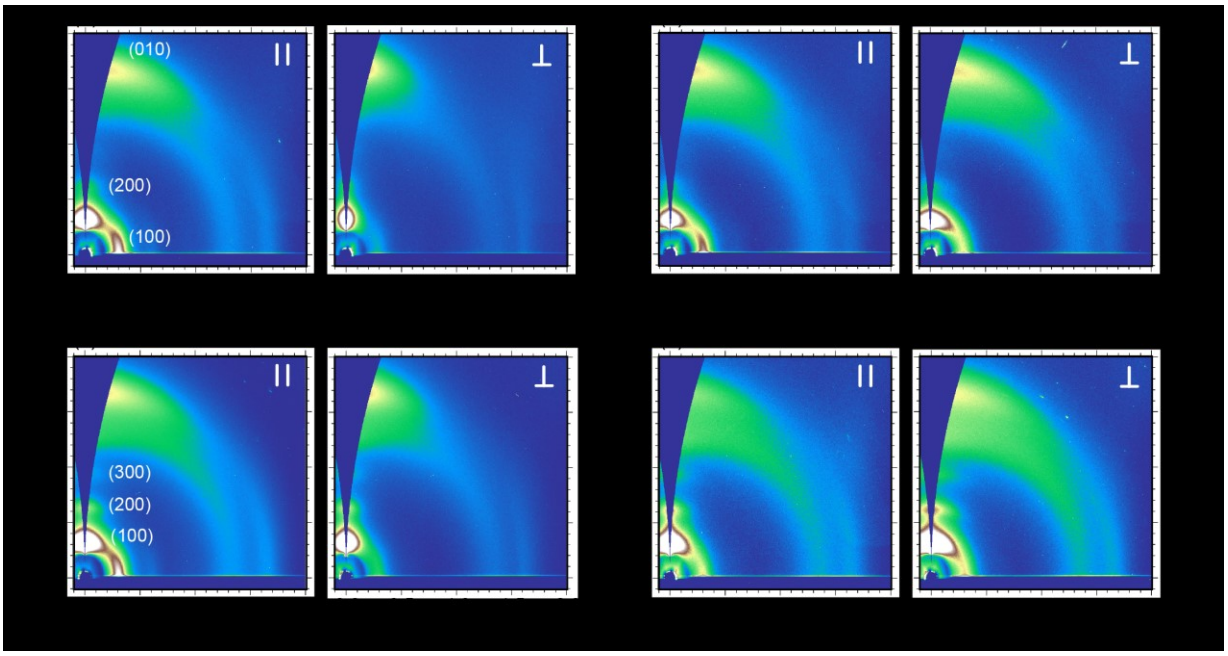

Figure 6. 2D GIWAXS images for the strained 30 nm thick PDPP-4T films with X-ray beam nominally parallel (∥) and perpendicular (⊥) to the strain direction. (a) A 60 % strained film. (b) The film strained to 60 % and released back to 20 % strain. (c) A film cyclically strained 100 times between 20 % and 60 % strain and held at the 60 % strain state. (d) A film cyclically strained 100 times and held at the 20 % strain state.

2.4 Charge Transport Behavior

Finally, charge mobility was measured in the strained films. In this case, we consider the 30 nm thick films strained on untreated PDMS and then transfer printed onto bottom-gate bottom-contact organic field effect transistors (OFETs). The saturated field effect charge mobility was extracted from the OFET transfer curves, with typical curves given in **Figure 7**. The charge mobility of the unstrained PDPP-4T was measured to be 0.15 ± 0.04 $cm^2 V^{-1} s^{-1}$. In 60 % strained film, the charge mobility along the direction of strain remained similar at 0.14 ± 0.01 $cm^2 V^{-1} s^{-1}$, while the charge mobility in the transverse direction decreased to 0.05 ± 0.01 $cm^2 V^{-1} s^{-1}$. When the strain was released to 20 %, the charge mobility in the direction of strain was 0.15 ± 0.03 cm^2

V^{-1} s^{-1}, and in the transverse direction was 0.12 ± 0.04 cm^2 V^{-1} s^{-1}. Further strain cycle measurements were not measured due to the appearance of delamination in cyclically strained films on untreated PDMS. Measurements were not made on UVO treated PDMS due to the inability to transfer print the films onto the transistor test beds. Nevertheless, these results are consistent with the average orientation of the backbone in the strained films. Charge mobility tracking with polymer backbone orientation has been found in previous demonstrations of cyclically strained polymer semiconductors.[13,16] This includes retaining a similar charge mobility in the direction on polymer alignment in the strained DPP based polymers.[8,13]

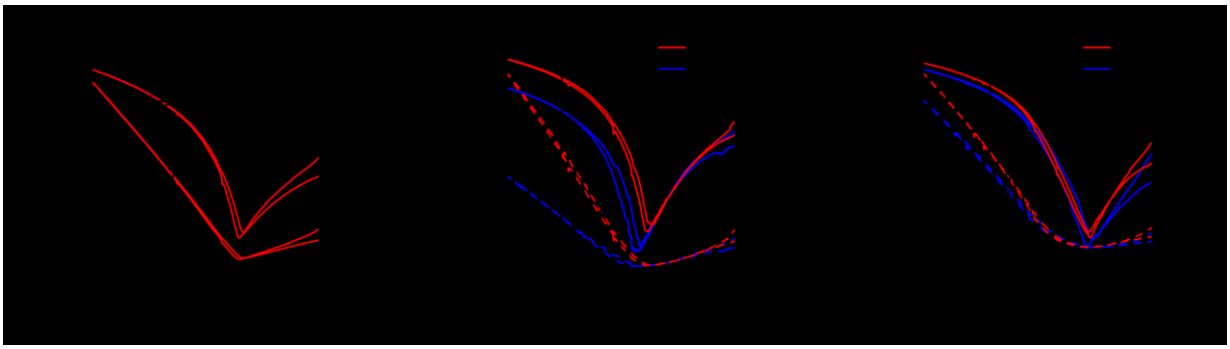

Figure 7. OFET transfer curves with drain current (I_D) vs. gate voltage (V_G) for (a) an unstrained 30 nm thick PDPP-4T film, (b) a 60 % strained film with curves measured for charge transport parallel (para.) and perpendicular (perp.) to the strain direction, and (c) a film strained to 60 % strain and released to 20 % strain for charge transport parallel and perpendicular to the strain direction. The curves include forward and backward voltage sweeps to capture hysteresis.

3. Conclusion

By managing the adhesion, stiffness mismatch between the film and substrate, and the effective strain range the composite sees during operation, plastic deformation of viscoelastic polymers has been shown to be a viable approach to achieve intrinsically stretchable organic

electronics. In particular, when a highly strained film/elastomer composite is released, the film may wrinkle, fold, delaminate, or plastically deform. Plastic deformation of the thin film can be favored over wrinkling due to synergistic effects of lower film stiffness and yield strength combined with increased substrate stiffness. In addition, improving the adhesion between the film and elastomer substrate reduces the competing failure mechanism of film delamination. Taking these factors into account, it was shown that PDPP-4T films could be cyclically strained over a nominal 40 % strain range for 100 strain cycles with minimal changes to the surface topography. It was shown that over this strain range, the film is plastically deforming and the polymer backbone orients in the direction of applied strain. While the polymer chains are orienting with strain, the packing order of the polymer was found to be largely stable with similar aggregation and X-ray diffraction characteristics. The stable morphological changes with applied strain resulted in predictable changes in charge transport where charge mobility tracked well with in-plane polymer orientation.

This study considered a simple 2-layer system using UVO treated PDMS as the substrate modifier. Translating these findings to stretchable devices require strategies where the elastomer adhesion and modulus are tuned in a long-term stable manner. Adhesion may be tuned through carefully designed monolayers that are grafted onto the elastomer,[37] whereas the stiffness may be tuned through appropriate elastomer selection or possible through nano-composite strategies.[38] In addition, for devices that include multiple heterogeneous layers careful design of the elasticity and adhesion of each component must be considered carefully to realize fully functional devices. Nevertheless, this work highlights that neat polymer semiconductor films that can deform significantly in tension are promising candidates for intrinsically stretchable semiconductors that must be stable under cyclic strain if interfaces are appropriately managed.

4. Experimental Section

Materials and processing: The PDPP-4T was purchased from Ossila, Ltd, with a number average molecular weight M_n = 76.2 kg mol^{-1}, and a polydispersity of 2.45.[57] The PDPP-4T film was dissolved in chloroform at 4 mg ml^{-1} and 8 mg ml^{-1} to achieve the 30 nm and 150 nm thick films, respectively. The solution was spun cast onto octyltrichlorosilane (OTS) treated Si substrate at 1500(2π) rad min^{-1} (1500 rpm) for 30 s at room temperature, followed by annealing at 150 ºC for 15 min. The films were then transferred onto the PDMS substrates using a previously described process.[14,58] Breifly, the PDMS is laminated to the film with very little pressure followed by quick withdrawal of the PDMS resulting in film transfer from the Si substrate to the PDMS. We have used this method widely to produce films with consistent mechanical and electrical properties.[14,47,58] The strain process was done by motorized strain stage with the strain rate of approximately 5 % s^{-1}. The strain rate was kept constant between samples to avoid the dependence of strain rate on the mechanical behavior of the composite. The PDMS (Sylgard 184) was prepared at 15:1 base to cross-linking ratio and cured in a vacuum oven held at 85 kPa at 60 ºC over a period of ≈ 12 h. The UVO treatment consisted of placing a free-standing PDMS slab into a UVO chamber (Jelight, model No. 42) that is in a fume hood and treating the PDMS for 10 min or 20 min. The lamp intensity is 28 mW/m^2 with a lamp to sample distance of 6 mm.

Film characterization: UV-visible spectroscopy measurements were made using an Ocean Optics Jazz spectrometer. The AFM images were measured using an Asylum MFP-3D-BIO in tapping mode. In both cases, the measurements were conducted while the film was on a PDMS substrate. GIWAXS measurements were performed at the Stanford Synchrotron Radiation Lightsource (SSRL) on beamline 11-3 with an X-ray energy of 12.735 keV, and an incidence

angle of ≈0.12°. The scattering was recorded on a MAR CCD225 detector. The instrument was calibrated using a LaB_6 crystal standard. For X-ray measurements, the films were strained on 20 min UVO PDMS and transferred onto Si substrates. Elastic contraction of the strained films was measured by first straining the films by 50 % while on a PDMS substrate. The films were then transfer printed to a poly(styrenesulfonate) (PSS) coated glass slides and the film length was recorded. After transfer printing the PDPP-4T film, water was added gently onto the sample. The PDPP-4T film then floats off the substrate. The film is left in the water bath for approximately 5 min to ensure the PSS is fully removed. The film is then picked up on a clean silicon substrate and its final length is recorded. The PSS was cast onto clean glass slides from 1 % solution in water at 4000(2π) rad min^{-1} (4000 rpm), followed by thermally annealing at 100 ^{o}C for 10 min.

Mechanical and electrical characterization: Crack onset strain of the DPP-4T films was determined by straining the film on the PDMS susbtrate and monitoring for cracks visual with an optical microscope. Wrinkle onset strain was measured by probing the film surface by AFM with increasing successive strain cycles. The film is strained to a specified extend then the strain is removed. The film on elastomer, while being held in the stain stage, is placed under the AFM probe tip. The wrinkle onset strain was measured for 3 films for all cases. The wrinkle onset strain was found to be within 2% strain of the average value, and this is given as the uncertainty for all cases. Peel tests were performed using an Instron 5943 tensile tester. The PDPP-4T films where held on a PDMS slab, which was adhered to a glass substrate. Scotch magic tape® was laminated onto the PDPP-4T film surface and attached to the arm of the tensile tester. A perpendicular force was applied on the tape to delaminate PDPP-4T from the PDMS substrate. The force and displacement were recorded, and the period over which the applied force is stable is used to determine adhesion energy. The adhesion energy (Γ_c) was calculated by $\Gamma_c = F/w$,

where F is average peel force, and w is the width of tape.[59] The transistor tests beds were fabricated by thermally evaporating Ti/Au (4 nm/35 nm) electrodes onto highly doped p-type Si wafer with 300 nm SiO_2 gate dielectric. The OTFT channel lengths were 80 μm and 100 μm and channel width was 1000 μm, patterned by photolithography. Transfer characteristics were measured with gate voltage swept from +20 V to −60 V with a −60 V source voltage. Saturated mobility was calculated by using linear fit of the square root of the source-drain current versus the gate voltage. The uncertainty was estimated by taking one standard deviation of a minimum of 4 devices.

ASSOCIATED CONTENT

Supporting Information.

Dynamic mechanical analysis data, ellipsometry data, GIWAXS line scans, AFM images and UV-visible spectroscopy data of stretched films.

AUTHOR INFORMATION

Corresponding Author

E-mail: btoconno@ncsu.edu

ACKNOWLEDGMENT

This research work was supported by the National Science Foundation award CMMI-1554322 and CMMI-1728370. X-ray diffraction was carried out at the Stanford Synchrotron Radiation Lightsource, a national user facility operated by Stanford University on behalf of the U.S. Department of Energy, Office of Basic Energy Sciences. The authors would like to thank the Y.

Zhu group for assistance with contact angle measurement, the M. Dickey group for assistance with peel tests.

References

(1) Rogers, J. A.; Someya, T.; Huang, Y. G. Materials and Mechanics for Stretchable Electronics. *Science* **2010**, *327*, 1603–1607.

(2) Kim, H. J.; Sim, K.; Thukral, A.; Yu, C. Rubbery Electronics and Sensors from Intrinsically Stretchable Elastomeric Composites of Semiconductors and Conductors. *Sci. Adv.* **2017**, *3*, e1701114.

(3) Choi, W. M.; Song, J.; Khang, D.; Jiang, H.; Huang Y. Y.; Rogers, J. A.; Biaxliaaly Stretchable "Wavy" Silicon Nanomemranes. *Nano Lett.* **2007**, *7*, 1655-1663.

(4) Lv, C.; Yu, H.; Jiang, H.; Archimedean Spiral Design for Extremely Stretchable Interconnects. *Extreme Mech. Lett.* **2014**, *1*, 29-34.

(5) Xu, J.; Wang, S.; Wang, G. J. N.; Zhu, C.; Luo, S.; Jin, L.; Gu, X.; Chen, S.; Feig, V. R.; To, J. W. F.; Rondeau-Gagné, S.;, Park, J.; Schroeder, B. C.; Lu, C. Oh, J.; Wang, Y.; Kim, Y.; Yan, H.; Sinclair, R.; Zhou, D.; Xue, G.; Murmann, B.; Linder, C.; Cai, W.; Tok, J. B.; Chung, J.; Bao, Z. Highly Stretchable Polymer Semiconductor Films through the Nanoconfinement Effect. *Science* **2017**, *355,* 6320.

(6) Shin, M.; Oh, J. Y.; Byun, K. E.; Lee, Y. J.; Kim, B.; Baik, H. K.; Park, J. J.; Jeong, U. Polythiophene Nanofibril Bundles Surface-Embedded in Elastomer: A Route to a Highly Stretchable Active Channel Layer. *Adv. Mater.* **2015**, *27*, 1255–1261.

(7) Zhang, G.; McBride, M.; Persson, N.; Lee, S.; Dunn, T. J.; Toney, M. F.; Yuan, Z.; Kwon, Y. H.; Chu, P. H.; Risteen, B.; Reichmanis, E. Versatile Interpenetrating Polymer Network Approach to Robust Stretchable Electronic Devices. *Chem. Mater.* **2017**, *29*, 7645–7652.

(8) Young Oh, J.; Rondeau-Gagné, S.; Chiu, Y.-C.; Chortos, A.; Lissel, F.; Nathan Wang, G.-J.; Schroeder, B. C.; Kurosawa, T.; Lopez, J.; Katsumata, T.; et al. Intrinsically Stretchable and Healable Semiconducting Polymer for Organic Transistors. *Nature* **2016**, *539*, 411–415.

(9) Nathan Wang, G.-J.; Shaw, L.; Xu, J.; Kurosawa, T.; Schroeder, B. C.; Oh, J. Y.; Benight, S. J.; Bao, Z. Inducing Elasticity through Oligo-Siloxane Crosslinks for Intrinsically Stretchable Semiconducting Polymers. *Adv. Funct. Mater.* **2016**, *26*, 7254–7262.

(10) Savagatrup, S.; Printz, A. D.; O'Connor, T. F.; Zaretski, A. V; Lipomi, D. J. Molecularly Stretchable Electronics. *Chem. Mater.* **2014**, *26*, 3028–3041.

(11) Scott, J. I.; Xue, X.; Wang, M.; Kline, R. J.; Hoffman, B.; Dougherty, D.; Zhou, C.; Bazan, G. C.; O'Connor, B. T. Significantly Increasing the Ductility of High Performance Polymer Semiconductors through Polymer Blending. *ACS Appl. Mater. Interfaces* **2016**, *8*, 14037–14045.

(12) Chortos, A.; Lim, J.; To, J. W. F.; Vosgueritchian, M.; Dusseault, T. J.; Kim, T. H.; Hwang, S.; Bao, Z. A. Highly Stretchable Transistors Using a Microcracked Organic Semiconductor. *Adv. Mater.* **2014**, *26*, 4253–4259.

(13) Lu, C.; Lee, W. Y.; Gu, X.; Xu, J.; Chou, H. H.; Yan, H.; Chiu, Y. C.; He, M.; Matthews,

J. R.; Niu, W.; Tok, J. B.; Toney, M. F.; Chen, W.; Bao, Z.; Effects of Molecular Structure and Packing Order on the Stretchability of Semicrystalline Conjugated Poly(Tetrathienoacene-Diketopyrrolopyrrole) Polymers. *Adv. Electron. Mater.* **2017**, *3*, 1600311.

(14) O'Connor, B.; Kline, R. J.; Conrad, B. R.; Richter, L. J.; Gundlach, D.; Toney, M. F.; DeLongchamp, D. M. Anisotropic Structure and Charge Transport in Highly Strain-Aligned Regioregular Poly(3-Hexylthiophene). *Adv. Funct. Mater.* **2011**, *21*, 3697–3705.

(15) Wu, H. C.; Benight, S. J.; Chortos, A.; Lee, W. Y.; Mei, J. G.; To, J. W. F.; Lu, C. E.; He, M. Q.; Tok, J. B. H.; Chen, W. C.; Bao, Z.; A Rapid and Facile Soft Contact Lamination Method: Evaluation of Polymer Semiconductors for Stretchable Transistors. *Chem. Mater.* **2014**, *26*, 4544–4551.

(16) Sun, T.; Scott, J. I.; Wang, M.; Kline, R. J.; Bazan, G. C.; O'Connor, B. T. Plastic Deformation of Polymer Blends as a Means to Achieve Stretchable Organic Transistors. *Adv. Electron. Mater.* **2017**, *3*, 1600388.

(17) Printz, A. D.; Savagatrup, S.; Burke, D. J.; Purdy, T. N.; Lipomi, D. J. Increased Elasticity of a Low-Bandgap Conjugated Copolymer by Random Segmentation for Mechanically Robust Solar Cells. *Rsc Adv.* **2014**, *4*, 13635–13643.

(18) Son, S. Y.; Kim, J. H.; Song, E.; Choi, K.; Lee, J.; Cho, K.; Kim, T. S.; Park, T. Exploiting π-π Stacking for Stretchable Semiconducting Polymers. *Macromolecules* **2018**, *51*, 2572–2579.

(19) Wen, H. F.; Wu, H. C.; Aimi, J.; Hung, C. C.; Chiang, Y. C.; Kuo, C. C.; Chen, W. C.

Soft Poly(Butyl Acrylate) Side Chains toward Intrinsically Stretchable Polymeric Semiconductors for Field-Effect Transistor Applications. *Macromolecules* **2017**, *50*, 4982–4992.

(20) O'Connor, B. T.; Awartani, O. M.; Balar, N. Morphological Considerations of Organic Electronic Films for Flexible and Stretchable Devices. *MRS Bulletin*. **2017**, *42*, 108–114.

(21) Savagatrup, S.; Chan, E.; Renteria-Garcia, S. M.; Printz, A. D.; Zaretski, A. V; O'Connor, T. F.; Rodriquez, D.; Valle, E.; Lipomi, D. J. Plasticization of PEDOT:PSS by Common Additives for Mechanically Robust Organic Solar Cells and Wearable Sensors. *Adv. Funct. Mater.* **2015**, *25*, 427–436.

(22) Ha, J. S.; Kim, K. H.; Choi, D. H. 2,5-Bis(2-Octyldodecyl)Pyrrolo[3,4-c]Pyrrole-1,4-(2H,5H)-Dione-Based Donor-Acceptor Alternating Copolymer Bearing 5,5-Di(Thiophen-2-Yl)-2, 2-Biselenophene Exhibiting 1.5 $cm^2V^{-1}S^{-1}$ Hole Mobility in Thin-Film Transistors. *J. Am. Chem. Soc.* **2011**, *133*, 10364–10367.

(23) Li, Y.; Sonar, P.; Singh, S. Annealing-Free High-Mobility Diketopyrrolopyrrole−Quaterthiophene Copolymer for Solution-Processed Organic Thin Film Transistors. *J. Am. Chem. Soc.* **2011**, 2198–2204.

(24) Sun, B.; Hong, W.; Aziz, H.; Abukhdeir, N. M.; Li, Y.; Sun; Hong, W.; Aziz, H.; Abukhdeir, N. M.; Li, Y. Dramatically Enhanced Molecular Ordering and Charge Transport of a DPP-Based Polymer Assisted by Oligomers through Antiplasticization. *J. Mater. Chem. C* **2013**, *1*, 4423–4426.

(25) Chung, J. Y.; Nolte, A. J.; Stafford, C. M. Surface Wrinkling: A Versatile Platform for

Measuring Thin-Film Properties. *Adv. Mater.* **2011**, *23*, 349–368.

(26) Chung, J. Y.; Lee, J. H.; Beers, K. L.; Stafford, C. M. Stiffness, Strength, and Ductility of Nanoscale Thin Films and Membranes: A Combined Wrinkling-Cracking Methodology. *Nano Lett.* **2011**, *11*, 3361–3365.

(27) Efimenko, K.; Wallace, W. E.; Genzer, J. Surface Modification of Sylgard-184 Poly(Dimethyl Siloxane) Networks by Ultraviolet and Ultraviolet/Ozone Treatment. *J. Colloid Interface Sci.* **2002**, *254*, 306–315.

(28) Özçam, A. E.; Efimenko, K.; Genzer, J. Effect of Ultraviolet/Ozone Treatment on the Surface and Bulk Properties of Poly(Dimethyl Siloxane) and Poly(Vinylmethyl Siloxane) Networks. *Polym.* **2014**, *55*, 3107–3119.

(29) Berdichevsky, Y.; Khandurina, J.; Guttman, A.; Lo, Y. H. UV/Ozone Modification of Poly(Dimethylsiloxane) Microfluidic Channels. *Sensors Actuators, B Chem.* **2004**, *97*, 402–408.

(30) Béfahy, S.; Lipnik, P.; Pardoen, T.; Nascimento, C.; Patris, B.; Bertrand, P.; Yunus, S. Thickness and Elastic Modulus of Plasma Treated PDMS Silica-like Surface Layer. *Langmuir* **2010**, *26*, 3372–3375.

(31) Ouyang, M.; Yuan, C.; Muisener, R. J.; Boulares, A.; Koberstein, J. T. Conversion of Some Siloxane Polymers to Silicon Oxide by UV/Ozone Photochemical Processes. *Chem. Mater.* **2000**, *12*, 1591–1596.

(32) Wang, Z.; Volinsky, A. A.; Gallant, N. D.; Crosslinking Effect on Polydimethylsiloxane Elastic Modulus Measured. *J. Appl. Polym. Sci.* **2014**, *131*, 41050.

(33) Efimenko, K.; Rackaitis, M.; Manias, E.; Vaziri, A.; Mahadevan, L.; Genzer, J. Nested Self-Similar Wrinkling Patterns in Skins. *Nat. Mater.* **2005**, *4*, 293–297.

(34) Bowden, N.; Huck, W. T. S.; Paul, K. E.; Whitesides, G. M. The Controlled Formation of Ordered, Sinusoidal Structures by Plasma Oxidation of an Elastomeric Polymer. *Appl. Phys. Lett.* **1999**, *75*, 2557–2559.

(35) Balar, N.; O'Connor, B. T. Correlating Crack Onset Strain and Cohesive Fracture Energy in Polymer Semiconductor Films. *Macromolecules* **2017**, *50*, 8611–8618.

(36) Kim, H.; Yoon, B.; Sung, J.; Choi, D.-G.; Park, C. Micropatterning of Thin P3HT Films via Plasma Enhanced Polymer Transfer Printing. *J. Mater. Chem.* **2008**, *18*, 3489-3495.

(37) Genzer, J.; Bhat, R. R.; Surface-Bound Soft Matter Gradients. *Langmuir*, **2008**, *24*, 2294-2317.

(38) Liff, S. M.; Kumar, N.; McKinley, G. H.; High-Performance Elastomeric Nanocomposites via Solvent-Exchange Processing. *Nat. Mater.* **2007**, *6*, 76-83.

(39) Lipomi, D. J.; Tee, B. C. K.; Vosgueritchian, M.; Bao, Z. N. Stretchable Organic Solar Cells. *Adv. Mater.* **2011**, *23*, 1771-1775.

(40) Nolte, A. J.; Chung, J. Y.; Davis, C. S.; Stafford, C. M.; Wrinkling-to-Delamination Transition in Thin Polymer Films on Compliant Substrates. *Soft Matter*, **2017**, *13*, 7930-7937.

(41) Printz, A. D.; Zaretski, A. V.; Savagatrup, S.; Chiang, A. S. C.; Lipomi, D. J. Yield Point of Semiconducting Polymer Films on Stretchable Substrates Determined by Onset of Buckling. *ACS Appl. Mater. Interfaces* **2015**, *7*, 23257–23264.

(42) Ebata, Y.; Croll, A. B.; Crosby, A. J.; Wrinkling and Strain Localizations in Polymer Thin Films. *Soft Matter*, **2012**, *8*, 9086-9091.

(43) Chung, J. Y.; Douglas, J. F.; Stafford, C. M.; A Wrinkling-Based Method for Investigating Glassy Polymer Film Relaxation as a Function of Film Thickness and Temperature. *J. Chem. Phys.* **2017**, *147*, 154902.

(44) Ayoub, G.; Zaïri, F.; Naït-Abdelaziz, M.; Gloaguen, J. M. Modelling Large Deformation Behaviour under Loading-Unloading of Semicrystalline Polymers: Application to a High Density Polyethylene. *Int. J. Plast.* **2010**, *26*, 329–347.

(45) Senden, D. J. A.; Van Dommelen, J. A. W.; Govaert, L. E. Strain Hardening and Its Relation to Bauschinger Effects in Oriented Polymers. *J. Polym. Sci. Part B Polym. Phys.* **2010**, *48*, 1483–1494.

(46) Roth, B.; Savagatrup, S.; de los Santos, N. V; Hagemann, O.; Carle, J. E.; Helgesen, M.; Livi, F.; Bundgaard, E.; Sondergaard, R. R.; Krebs, F. C.; Lipomi, D. J.; Mechanical Properties of a Library of Low-Band-Gap Polymers. *Chem. Mater.* **2016**, *28*, 2363–2373.

(47) Awartani, O. M.; Zhao, B. X.; Currie, T.; Kline, R. J.; Zikry, M. A.; O'Connor, B. T. Anisotropic Elastic Modulus of Oriented Regioregular Poly(3-Hexylthiophene) Films. *Macromolecules* **2016**, *49*, 327–333.

(48) Duckett, R. A.; Ward, I. M.; Zihlif, A. M. Direct Measurements of the Reverse Stress Asymmetry in the Yielding of Anisotropic Polypropylene. *Journal of Materials Science*. **1972**, 480–482.

(49) Urayama, K.; Kawamura, T.; Kohjiya, S. Structure-Mechanical Property Correlations of

Model Siloxane Elastomers with Controlled Network Topology. *Polymer*. **2009**, *50*, 347–356.

(50) Mitchell, M. R.; Link, R. E.; Brieu, M.; Diani, J.; Bhatnagar, N. A New Biaxial Tension Test Fixture for Uniaxial Testing Machine—A Validation for Hyperelastic Behavior of Rubber-like Materials. *J. Test. Eval.* **2007**, *35*, 100688.

(51) Lu, N.; Wang, X.; Suo, Z.; Vlassak, J. Metal Films on Polymer Substrates Stretched beyond 50%. *Appl. Phys. Lett.* **2007**, *91, 221909*.

(52) Sawyer, E. J.; Zaretski, A. V; Printz, A. D.; De los Santos, N. V; Bautista-Gutierrez, A.; Lipomi, D. J. Large Increase in Stretchability of Organic Electronic Materials by Encapsulation. *Extrem. Mech. Lett.* **2016**, *8*, 78-87.

(53) Read, D. T.; Volinsky, A.; Measurements for Mechanical Reliability of Thin Films. *Meas. Mech. Reliab. Thin Film.* **2009**, 337–358.

(54) Liu, F.; Gu, Y.; Wang, C.; Zhao, W.; Chen, D.; Briseno, A. L.; Russell, T. P. Efficient Polymer Solar Cells Based on a Low Bandgap Semi-Crystalline DPP Polymer-PCBM Blends. *Adv. Mater.* **2012**, *24*, 3947–3951.

(55) Zhao, B. X.; Awartani, O.; O'Connor, B.; Zikry, M. A. Microstructural Behavior and Failure Mechanisms of Organic Semicrystalline Thin Film Blends. *J. Polym. Sci. Part B-Polymer Phys.* **2016**, *54*, 896–907.

(56) Baker, J. L.; Jimison, L. H.; Mannsfeld, S.; Volkman, S.; Yin, S.; Subramanian, V.; Salleo, A.; Alivisatos, A. P.; Toney, M. F. Quantification of Thin Film Crystallographic Orientation Using X-Ray Diffraction with an Area Detector. *Langmuir* **2010**, *26*, 9146–

9151.

57) Certain commercial equipment or materials are identified in this paper in order to specify the experimental procedure adequately. Such identification is not intended to imply recommendation or endorsement by the National Institute of Standards and Technology.

(58) Sen, P.; Xiong, Y.; Zhang, Q.; Park, S.; You, W.; Ade, H.; Kudenov, M. W.; O'Connor, B. T.; Shear-Enhanced Transfer Printing of Conducting Polymer Thin Films. *ACS Appl. Mater. Interfaces*, **2018**, *10*, 31560-31567.

(59) Kendall, K. Thin-Film Peeling-the Elastic Term. *J. Phys. D. Appl. Phys.* **1975**, *8* (13), 1449–1452.

Table of Content